

Ferromagnetic Domain Structure of $\text{La}_{0.78}\text{Ca}_{0.22}\text{MnO}_3$ Single Crystals

G. Jung,^{1,2} V. Markovich,¹ C. J. van der Beek,² D. Mogilyansky,³ and Ya. M. Mukovskii⁴

¹*Department of Physics, Ben Gurion University of the Negev,
P.O. BOX 653, 84105 Beer Sheva, Israel*

²*Laboratoire des Solides Irradiés, CNRS UMR 7642 & CEA/DSM/DRECAM,
Ecole Polytechnique, 91128 Palaiseau, France*

³*Institute of Applied Research, Ben Gurion University of the Negev,
P.O.Box 653, 84105 Beer Sheva, Israel*

⁴*Moscow State Steel and Alloys Institute, 119991, Moscow, Russia*

(Dated: March 25, 2021)

Abstract

The magneto-optical technique has been employed to observe spontaneous ferromagnetic domain structures in $\text{La}_{0.78}\text{Ca}_{0.22}\text{MnO}_3$ single crystals. The magnetic domain topology was found to be correlated with the intrinsic twin structure of the investigated crystals. With decreasing temperature the regular network of ferromagnetic domains undergoes significant changes resulting in apparent rotation of the domain walls in the temperature range of 70-150 K. The apparent rotation of the domain walls can be understood in terms of the Jahn-Teller deformation of the orthorhombic unit cell, accompanied by additional twinning.

PACS numbers: 75.47.Lx; 75.60.Ch

I. INTRODUCTION

The remarkable magnetic and transport properties of the mixed-valence manganese perovskites of the form $R_{1-x}A_x\text{MnO}_3$, where R is a rare-earth ion and A is a divalent ion, continuously attract attention of many research groups. The central feature is a huge decrease in resistivity on application of a magnetic field, referred to as the colossal magneto-resistance (CMR) effect.^{1,2} The properties of CMR manganites strongly depend on the doping level x . In the $\text{La}_{1-x}\text{Ca}_x\text{MnO}_3$ (LCMO) system the critical doping level $x = x_C = 0.225$ separates a nominally ferromagnetic (FM) insulating and orbitally ordered ground state from a ground state with a FM metallic character.^{1,2,3} There is convincing experimental evidence that the low temperature ground state of the LCMO system within the low doping range, $0.17 < x < 0.25$, contains distinct FM insulating and FM metallic phases.^{4,5,6} At temperatures below the magnetic ordering temperature T_C , the resistivity of the manganites doped with $x < x_C$ initially decreases, but with further temperature decrease it increases again.

It is generally agreed that electrical resistance of magnetic domain walls influences transport properties and magnetoresistance of classical ferromagnets and CMR manganites.⁷ Topology of the magnetic domains may therefore play a role in the temperature dependence of the resistivity even if no consensus has been reached both on the experimental observability of the domain-wall scattering and on the nature of the domain wall scattering mechanism.⁷ The topology of magnetic domains results from the minimalization of the system free energy and is related to the magnetic anisotropy of the host material. Surprisingly, still little is known about the structure and properties of the spontaneous domains in CMR perovskite single crystals.⁸

Magnetic domains in CMR manganites can be efficiently investigated in-situ by means of the magneto-optical technique (MO). The non-invasive MO allows for monitoring the evolution of magnetic domains in large areas of the sample as a function of changing experimental parameters. In our recent report on magneto-optical investigations of magnetic domains in various LCMO crystals we have shown, among others, that the MO image of ferromagnetic Weiss domains can be easily confused with the contrast resulting from twin domains with different magnetic anisotropy.^{8,9}

Manganite LCMO crystals are intrinsically twinned in the process of crystallization. During cool-down they undergo a high temperature phase transition associated with lowering of

the symmetry.^{1,2} At room temperature LCMO has an orthorhombic structure (space group $Pnma$) with lattice parameters $a \approx \sqrt{2}a_p$, $b \approx 2a_p$, $c \approx \sqrt{2}a_p$, where a_p is the lattice parameter of a simple cubic perovskite. The long orthorhombic b axis can be directed along any one of the cubic axis. The a and c orthorhombic axes are perpendicular to b and rotated 45° with respect to the cubic axes. Depending on the direction of the b axis with respect to the cubic cell, three different orientations of the $Pnma$ unit cell are possible. Within each orientation a and c axis can be interchanged, leading to additional pair of twins. Domains with mutually perpendicular b axes, referred to as orthogonal twins, are preferentially separated by $\{110\}$ cubic planes. Twins with common b axis but with different a and c axis, so-called permutation twins, are separated by $\{100\}$ cubic planes.^{10,11}

In this paper we report on MO investigations of the spontaneous ferromagnetic domain structure in $\text{La}_{0.78}\text{Ca}_{0.22}\text{MnO}_3$ single crystals. In particular, we report on the striking change in the domain topology occurring in the temperature range 70-150 K. The results are interpreted in terms of additional twinning induced by a possible low temperature Jahn-Teller structural transition.

II. EXPERIMENTAL AND RESULTS

$\text{La}_{1-x}\text{Ca}_x\text{MnO}_3$ crystals were grown by a floating zone method using radiative heating.¹² The X-ray data for the $\text{La}_{0.78}\text{Ca}_{0.22}\text{MnO}_3$ crystal were compatible with the orthorhombic unit cell $a = 5.4951(5) \text{ \AA}$, $b = 7.7844(6) \text{ \AA}$, $c = 5.4947(6) \text{ \AA}$, of a perovskite structure. The as-grown crystal had form of a cylinder, about 4 cm long and 4 mm in diameter. For the MO investigations we have cut 0.5 mm thick wafers in the direction perpendicular to the as-grown cylindrical crystal axis and polished one of the flat surfaces to optical quality. Samples for resistive measurements were prepared in the form of small rectangular bars with vacuum evaporated gold contacts for standard four-point resistance measurements.

The crystallographic orientations of the crystal and wafers were determined by the Laue method with accuracy of $\pm 2^\circ$. The main cylindrical axis of the as-grown crystal was found to deviate 15° from the crystallographic $[110]$ cubic direction. The stereographic projection of the wafer plane is shown in Fig 1. The growth direction is indicated with a cross and the cubic symmetry crystallographic planes with circles.

For the magneto-optical imaging a ferrimagnetic garnet indicator film with in-plane

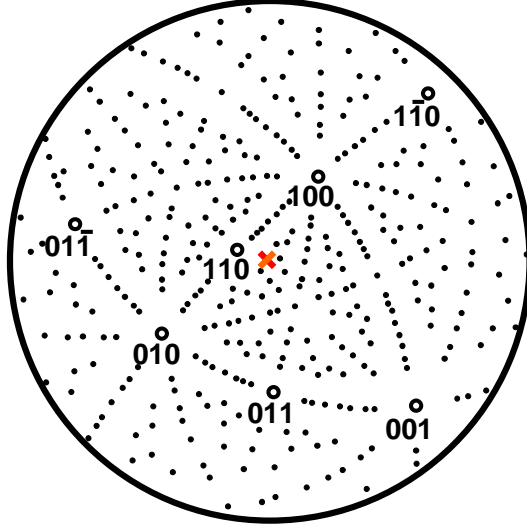


FIG. 1: The stereographic projection of the wafer plane on which the magnetic domain structure shown in Fig. 4 was observed. The growth direction is indicated with a cross. The cubic crystallographic planes are marked with circles.

anisotropy was placed directly on the top of the polished surface of the wafer and observed using linearly polarized light. The reflected light intensity, observed through an analyzer oriented nearly perpendicularly to the polarization direction of the incident light, corresponds to the local value of the magnetic induction component perpendicular to the crystal and to the garnet. To visualize ferromagnetic Weiss domains the sample was slowly cooled down below T_C in zero applied field. In zero field conditions the magnetic contrast is not perturbed by magnetic anisotropy effects, as discussed in details elsewhere.^{8,9}

Figure 2 shows the temperature dependence of the zero magnetic field resistivity of LCMO single crystals with $x = 0.18, 0.20,$ and 0.22 . The general behavior of the resistivity in investigated crystals is the same. With decreasing temperature the resistivity reaches a pronounced maximum related to the metal-insulator (M-I) transition at $T = T_{M-I}$. The temperature of the maximum is very close to Curie temperature determined from independent magnetization measurements. For $\text{La}_{0.78}\text{Ca}_{0.22}\text{MnO}_3$ $T_C = 189 \pm 1$ K, while $T_{M-I} = 186$ K.¹³ At temperatures below the magnetic ordering temperature the resistivity decreases in a metallic way with $d\rho/dT > 0$, although the absolute value of the resistivity is much higher than in common metals. With further temperature decrease the resistivity exhibits a shallow minimum followed by a strong low temperature upturn towards a second low-temperature maximum

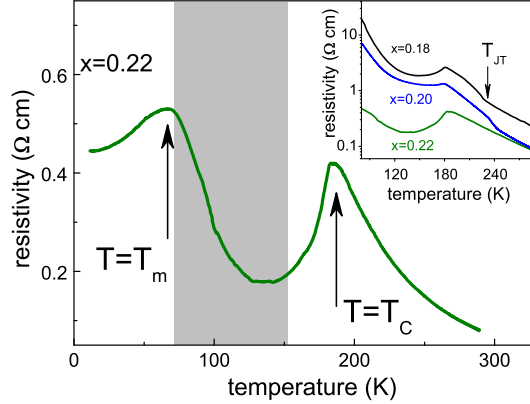


FIG. 2: Color on-line: Temperature dependence of the resistivity of $\text{La}_{0.78}\text{Ca}_{0.22}\text{MnO}_3$ crystal in zero applied magnetic field. The shaded area indicates the temperature range over which pronounced changes of the magnetic domain topology is observed. The evolution of the zero field resistivity of the $x = 0.22$ LCMO single crystal is confronted with those doped at $x = 0.18$ and 0.20 in the inset. Note that the step-like change of the resistivity in the paramagnetic phase in $x = 0.18$ and $x = 0.20$ crystals cannot be seen in $\text{La}_{0.78}\text{Ca}_{0.22}\text{MnO}_3$

which for $x = 0.22$ appears at $T_m \approx 68$ K. The independent magnetization measurements of our sample did not reveal any peculiarities at temperatures below T_C , suggesting that in the investigated temperature range there is only one magnetic transition at $T = T_C$.

Double maxima in the $R(T)$ dependence were previously observed in $\text{La}_{2/3}\text{Ca}_{1/3}\text{MnO}_{3-d}$ thin films with artificial grain boundaries playing the role of magnetic tunnel junctions.¹⁴ The low temperature resistivity peak in such films was attributed to spin-polarized tunnelling across grain boundaries. Recently a double peak feature was also observed in optimally doped LCMO single crystals.¹⁵ However, in single crystalline samples there are no grain boundaries and possible barriers for spin-polarized tunnelling may be associated with domain walls pinned to twin boundaries.⁷ Twin domain boundaries in CMR manganites single crystals play a role similar to that of grain boundaries in polycrystalline samples.^{6,15} Due to strong band bending at the boundary the carrier concentration is depleted and the temperature of the local M-I transition is depressed.^{14,15,16,17} The low temperature peak in the existing literature is thus interpreted as being due to local M-I transitions occurring at lower temperature than those in the sample bulk.^{14,15,16,17} Note that the double peak resistivity structure can be observed only in samples with low specific resistance at low temperatures, such that relatively low second maximum is not obscured by other resistivity contributions

which strongly increase with decreasing temperature.³

Figure 3a shows a MO micrograph of the polished surface of the $x = 22$ LCMO crystal taken after a slow cooling process down to 160 K in zero applied magnetic field. As we have pointed out in our earlier paper, these are the conditions under which unambiguous MO image of the Weiss domains can be obtained.⁸ The magnetic contrast associated with ferromagnetic domains appears immediately below T_C . The Weiss domains are revealed as zigzagging series of dark and bright stripes. The bright and dark regions in the MO image correspond to areas with opposite perpendicular component of the stray field, caused by opposite directions of the spontaneous magnetization in adjacent domains.⁸ The domains boundaries follow the intersections of (011) and (01 $\bar{1}$) planes with the crystal surface, as it can be deduced from the schematics shown on Fig. 3c. According to the crystallographic analysis (011) and (01 $\bar{1}$) planes separate structural orthogonal twin domains in which b axes are mutually perpendicular.¹⁸ If in one of the domains in Fig. 3 the b axis are directed along the [001] cubic orientation, then in the neighboring one they will be directed along the [010] cubic orientation. The applied magnetic field, up 500 Gauss, the maximum field available in our MO setup, does not change the domains orientation and neither modifies significantly their width.⁸ On the basis of the MO investigations we conclude that magnetic domain walls are pinned to the structural twin domain boundaries.

Temperature evolution of the shape of ferromagnetic domains in $\text{La}_{0.78}\text{Ca}_{0.22}\text{MnO}_3$ crystal is illustrated in Fig. 4 showing MO images of the crystal surface at various temperatures. With temperature decreasing below T_C the MO contrast increases, and the multi-stripe domain pattern becomes more and more pronounced. Simultaneously, the sample resistivity decreases due to increasing strength of the percolation of FM metallic domains, see Fig. 2. The width of an individual FM domain is in the range of 50 μm which is about half the width of the twin domains.^{8,9} The normal component of the domain surface magnetic field is in the range of 40 gauss.⁸ Such low values of the domain field, much below the expected saturation magnetization field are, at least partially, due do the presence of the conical closure domains, clearly seen as circular spots in the MO micrographs in Fig. 4 at temperatures close to T_C .

Below 150 K the domain structure starts to undergo significant changes. The smooth domain walls become corrugated and divide into segments separated by boundaries parallel to the intersection of the (001) planes with the crystal surface. The new domains extend in the direction orthogonal to the one dominating at higher temperatures. The width of

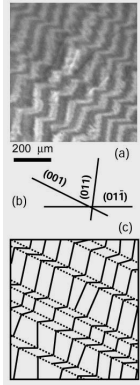


FIG. 3: a) MO image of the ferromagnetic domains observed in zero field cooled $\text{La}_{0.78}\text{Ca}_{0.22}\text{MnO}_3$ wafer at 165 K. b) Directions of intersections of the crystallographic planes with the wafer surface, as determined from the Laue analysis shown in Fig. 1. c) The schematics of the domain structure from the MO shown in a). For clarity of the picture the lines are drawn only along the domains with one direction of the spontaneous magnetization, which in the MO image appear as bright domains.

the domains extending in the perpendicular direction is much smaller than the width of the original ones. Eventually, as a result of such changes, the entire domain structure undergoes apparent rotation and elongates in the direction perpendicular to the original one. Changes in the domain structure end at temperatures around 70 K and are reversible. With increasing temperature the dominant direction of the ferromagnetic domains rotates back to the original one, the corrugation of the domain walls decreases and eventually disappears. The conical closure domains reappear in the MO images at temperatures close to T_C . However, in certain restricted areas of the sample, the domains do not fully return to their pristine state. The shape hysteresis is likely associated with strong pinning of the modified low temperature domain structure by localized defects. Nevertheless, heating of the crystal above T_C completely erases the memory of any frozen domain shapes.

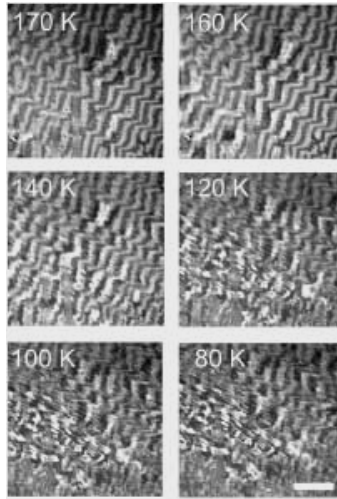


FIG. 4: Temperature evolution of the ferromagnetic domain structure as revealed by the MO imaging. The length of the white bar in the bottom right corner is 200 μm .

III. DISCUSSION

Our MO investigations suggest that the magnetic domain walls are pinned to the twin boundaries. Similar pinning phenomena are common in ferroelectric and ferromagnetic systems. Pinning of domain walls by twin boundaries has been observed in ferroelectric tetragonal perovskites¹⁹ and ferromagnetic alloys with martensitic structure.²⁰ A surface topography reflecting a twin structure coinciding with a micromagnetic domain structure was also observed in $\text{La}_{0.83}\text{Sr}_{0.13}\text{MnO}_{2.98}$ manganite single crystals.²¹

Any phase transition associated with lowering of the crystallographic symmetry generates crystallographic twins in the low-symmetry phase. It is therefore reasonable to assume that changes in the magnetic domain structure at temperatures below 150 K are due to additional twinning in the FM phase. The additional twins are directed perpendicularly to the major twins created at the high temperature cubic to orthorhombic transition. The appearance of additional perpendicular twin walls in our sample may be connected with the formation of permutation twins. We suggest that a possible origin of such excess twinning consists in lowering of the crystal symmetry by the cooperative Jahn-Teller (JT) transition occurring at low temperatures.

Structural transitions in manganites are invariably accompanied by additional microstructural strains at surfaces, grain boundaries, or twin planes.²² The strain fields affect spin orientation and magnetic domains will corrugate and elongate along the directions of the strain and/or additional twin walls. In $\text{La}_{1-x}\text{Sr}_x\text{MnO}_3$ (LSMO) system, which in the low doping regime ($x < x_C$) behaves very similar to the LCMO, the orthorhombic phase lattice parameters a and c are almost equal above the temperature of Jahn-Teller coherent distortion T_{JT} . As a result of the JT distortion a and c became significantly different and the c/a ratio sharply increases.^{23,24} Discrepancy between the lattice parameters leads to significant strain fields which may cause appearance of additional twins. Orthogonal D2 domains will divide into smaller permutation twins with twin boundaries directed along the [001] direction. Jahn-Teller transition in low doped LSMO lowers the crystal symmetry to monoclinic and even triclinic structure.^{24,25} A similar transition from the orthorhombic to the monoclinic phase in $\text{Sm}_{0.2}\text{Ca}_{0.8}\text{MnO}_3$ crystal was reported to result in the appearance of additional fine tweed-like domains in the monoclinic phase.²⁶

The stoichiometric lanthanum manganite LaMnO_3 at room temperature has an or-

thorhombic perovskite structure with the $Pnma$ space group symmetry and antiferrodistorsive orbital ordering (OO) of the Mn-O bond configuration.^{1,2} Alternating long and short Mn-O distances in the ac -plane are the signatures of orbital ordering resulting from the cooperative JT distortions. Below $T_{JT} \approx 750$ K the JT distortions are static resulting in O'- orthorhombic axial ratio $b/a < \sqrt{2}$, whereas above T_{JT} they are short ranged and give pseudocubic ratio $b/a \approx \sqrt{2}$, which is usually designated as O* - orthorhombic.²⁷ In both LCMO and LSMO systems the temperature of the O' - O* transition decreases sharply with increasing x .^{23,24,28,29,30} The cooperative JT effect is progressively suppressed, accompanied by developing ferromagnetism.¹⁰ For doping levels close to x_C the JT transition in both systems appears very close to T_C ,²⁸ or even below T_C .^{23,24,29,30}

One can see in Fig. 2 that the resistivities of $x = 0.18$ and $x = 0.2$ LCMO crystals exhibit a step-like feature in the $\rho(T)$ characteristics at $T_{JT} \approx 230 - 240$ K, commonly regarded as a hallmark of the JT transition.²⁸ Although we do not have a direct proof for the occurrence of the JT transition in $\text{La}_{0.78}\text{Ca}_{0.22}\text{MnO}_3$ crystal within the relevant temperature range, there are several indirect indications confirming such a hypothesis. Among them, the preliminary extended X-ray absorption fine structure measurements of our crystal have shown³¹ that Mn-O bond lengths and Jahn-Teller distortion parameter $\sigma_{JT} = \sqrt{1/3 \sum_i [(Mn-O)_i - \langle Mn-O \rangle]^2}$ change with temperature in a non-monotonic way not only in a close vicinity of T_C , as it has been reported previously for $x = 0.25$ LCMO,³² but also in the temperature range in which the topology of the magnetic domains changes.

Recent measurements of magnetic, transport, and thermal properties of low doped LCMO samples have shown that the JT transition in this system likely persists at doping levels above the percolation threshold, up to $x \approx 0.24$.²⁸ The shift to higher x in LCMO, with respect to LSMO, is caused by a smaller tolerance factor, which narrows the σ -band of electrons. Therefore, one may speculate that JT transition may also occur in our LCMO sample with $x = 0.22$.

The structural JT phase transition in LSMO with $x = 0.14$ occurs in the paramagnetic phase, $T_{JT} > T_C$, and is of the first order. At slightly higher doping level of $x = 0.15$, the structural phase transition appears in the ferromagnetic state at $T_{JT} < T_C$, and becomes of the second order.²⁹ A plausible reason for the absence of the step-like resistivity anomaly in the $\rho(T)$ characteristics of our sample may be the second order character of the JT transition in $x = 0.22$ LCMO.

Monoclinic distortions were found in low-doped LCMO with $x = 0.15$ ³³ and in the optimally doped, $x \sim 0.3$, epitaxial LCMO films and single crystals.^{15,34} Recently, high resolution X-ray diffraction and neutron powder diffraction structural investigation of low doped LCMO samples have established that for temperatures below x -dependent T_{JT} the symmetry changes from orthorhombic $Pnma$ to monoclinic $P2_1/c$.³⁵ The transition was directly revealed through observations of splitting of $(hk0)$ and (hkl) diffraction peaks, not allowed in the $Pnma$ space group. The JT transition to monoclinic structure was found to be accompanied by the loss of the mirror plane, signaling a new orbital ordering with two crystallographically independent Mn sites and a layer-type arrangement of the different MnO_6 octahedra along b axis. For $0.13 < x < 0.175$ the temperature variation of the unit cell volume exhibits a discontinuous change at $T = T_{JT}$ implying that JT transition is of the first order. However, when $x \geq 0.175$, the magnetic and structural characteristics vary smoothly through T_{JT} .³⁵ This corroborates our assumption that JT structural transition in $x = 0.22$ LCMO is of the second order.

The low temperature resistivity upturn in LCMO with $x = 0.18, 0.2$ is associated with strong competition between orbital ordered and orbital disordered ferromagnetic phases which results in cluster-glass freezing at $T \approx 70$ K.^{2,13} The cluster glass-like behavior manifests itself in strong frequency dependence of the ac susceptibility, remarkable rotation of the easy magnetization axis, and pronounced difference between zero field cooled and field cooled magnetization curves at the freezing temperature.^{13,36} With an exception of the rotation of an easy magnetization axis, remarkably less pronounced than in $x = 0.2$ sample, and very slight frequency dependence of the ac susceptibility, all cluster glass transition signatures are practically absent in $x = 0.22$ LCMO crystals.¹³ Nevertheless, while the real part of the ac-susceptibility of the $La_{0.78}Ca_{0.22}MnO_3$ crystal, see Fig. 5, does not show any spin glass peculiarities, the imaginary part χ'' exhibits a broad frequency dependent maximum in the temperature range 70 -140 K. The excess temperature dependent dissipation can be attributed to the motion of magnetic domain walls excited by the measuring ac magnetic field. Consistently with the scenario proposed in this paper, additional twinning leads to significant increase in the total length of the domain walls, what results in a broad χ'' peak.

The experiments show that the temperature range in which the domain topology changes coincides with the temperature range of the resistivity upturn, see Fig. 2. Can the low temperature resistivity be explained by the observed domain rotation? This is doubtlessly a

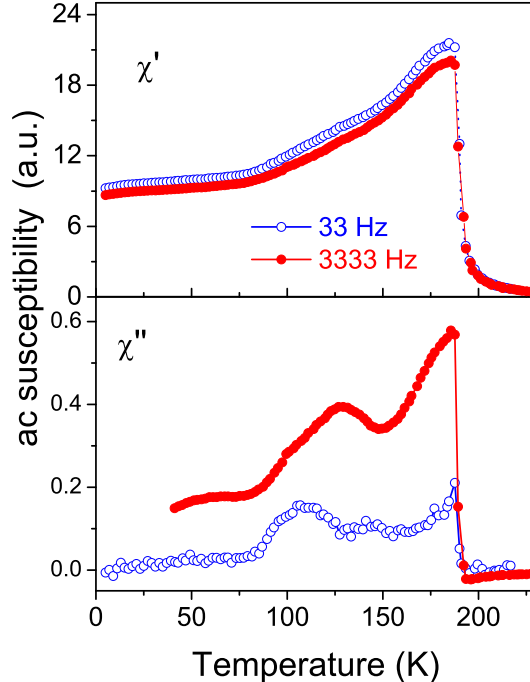


FIG. 5: Color on-line: The temperature dependence of the ac susceptibility, measured with 60 mOe ac field, does not exhibit pronounced cluster glass features, as observed previously in $x = 0.18$ and in $x = 0.20$ LCMO crystals. The quadrature component of the ac susceptibility shows a broad smeared maximum around 150 K, which we ascribe to the motion of additional domain walls excited by the ac field.

very attractive explanation. Nevertheless, one has to remember that a very similar behavior of the resistivity has been also observed in slightly less doped LCMO crystals with $x = 0.18$ and $x = 0.2$,^{6,36} in which the structural J-T transition occurs solely in the paramagnetic phase, $T_{JT} > T_C$.² We have associated the domain rotation with the structural J-T transition. Consistently, in these crystals, we have not detected any significant changes in the domain topology with changing temperature. Therefore, one has to conclude that even if the corrugated domain walls contribute to the observed resistivity upturn they cannot be accountable for the entire low temperature behavior of the resistivity which is likely due to action several interdependent factors.

In summary, transport measurements and magneto-optical imaging have been employed to study $\text{La}_{0.78}\text{Ca}_{0.22}\text{MnO}_3$ single crystal having the Ca-doping level close to the percolation threshold x_C . A prominent spontaneous magnetic domain structure in the form of zigzagging parallel stripes, with opposite direction of the spontaneous magnetization in adjacent

strips, appears in MO micrographs just below the Curie temperature $T_C = 189$ K. In the temperature range 70–150 K, corresponding to the low temperature resistivity upturn, a topological change in the domain structure occurs. The domain walls corrugate and eventually the entire domain structure rotates 90° with respect to the original direction. The evolution of the magnetic domain structure can be understood in terms of additional perpendicular twinning associated with a reduction of the crystal symmetry, from orthorhombic to monoclinic, due to a presumed low temperature cooperative Jahn-Teller transition.

Acknowledgments

This research was supported by the Israeli Science Foundation administered by the Israel Academy of Sciences and Humanities (grant 209/01) and by French-Israeli Arc-en-Ciel exchange program. Ya. M. M. acknowledges the support obtained from ISTC grant 1859.

-
- ¹ Colossal Magnetoresistive Oxides, ed. by Y. Tokura, Gordon and Breach Science Publishers, 2000.
 - ² J. B. Goodenough, Rare Earth-Manganese Perovskites, Handbook on the Physics and Chemistry of Rare Earth, vol. 33, ed. K. A. Gschneidner Jr., J. -C. G. Bunzli, and V. Pecharsky, Elsevier Science 2003.
 - ³ T. Okuda, Y. Tomioka, A. Asamitsu, and Y. Tokura, Phys. Rev. B **61**, 8009 (2000).
 - ⁴ G. Papavassiliou, M. Pissas, M. Belesi, M. Fardis, J. Dolinsek, C. Dimitropoulos, and J. P. Ansermet, Phys. Rev. Lett. **91**, 147205 (2003).
 - ⁵ G. Biotteau, M. Hennion, F. Moussa, J. Rodriguez-Carvajal, L. Pinsard, A. Revcolevschi, Y. M. Mukovskii, and D. Shulyatev, Phys. Rev. B **64**, 104421 (2001); M. Hennion, F. Moussa, P. Lehouelleur, F. Wang, A. Ivanov, Y. M. Mukovskii, and D. Shulyatev, Phys. Rev. Lett. **94**, 057006 (2005).
 - ⁶ Y. Yuzhelevski, V. Markovich, V. Dikovskiy, E. Rozenberg, G. Gorodetsky, G. Jung, D. A. Shulyatev, and Ya. M. Mukovskii, Phys. Rev. B **64**, 224428 (2001).
 - ⁷ M. Ziese, Rep. Prog. Phys. **65**, 143 (2002).
 - ⁸ G. Jung, M. Indenbom, V. Markovich, C. J. van der Beek, D. Mogilyansky, Ya. M. Mukovskii,

- J. Phys.: Cond. Matter, **16**, 5461 (2004).
- ⁹ G. Jung, V. Markovich, D. Mogilyansky, C. J. van der Beek, Ya. M. Mukovsky, J. Mag. Magn. Mat. **290-291P2**, 902 (2005).
- ¹⁰ B. B. Van Aken, A. Meetsma, Y. Tomioka, Y. Tokura, and T. T. M. Palstra, Phys. Rev. B **66**, 224414 (2002); B. B. Van Aken, Ph. D. Thesis, University of Groningen (2001), www.ub.rug.nl/eldoc/dis/science.
- ¹¹ G. Van Tendeloo, O. I. Lebedev, M. Hervieu and B. Raveau, Rep. Prog. Phys. **67**, 1315 (2004).
- ¹² D. Shulyatev, A. Arsenov, S. Karabashev, Ya. Mukovskii, J. Crystal Growth **198/199**, 511 (1999); D. Shulyatev, S. Karabashev, A. Arsenov, Ya. Mukovskii, S. Zverkov, J. Cryst. Growth **237-239**, 810 (2002).
- ¹³ V. Markovich, I. Fita, R. Puzniak, M. I. Tsindlekht, A. Wisniewski, and G. Gorodetsky, Phys. Rev. B **66**, 094409 (2002).
- ¹⁴ J. Klein, C. Hofener, S. Uhlenbruck, L. Alff, B. Buchner, and R. Gross, Europhys. Lett. **47**, 371 (1999).
- ¹⁵ B. I. Belevtsev, D. G. Naugle, K. D. D. Rathnayaka, A. Parasiris, and J. Fink-Finowicki, Physica B **355**, 341 (2005).
- ¹⁶ R. Gross, L. Alff, B. Büchner, B. H. Freitag, C. Höfener, J. Klein, Yafeng Lu, W. Mader, J. B. Philipp, M. S. R. Rao, P. Reutler, S. Ritter, S. Thienhaus, S. Uhlenbruck and B. Wiedenhorst, J. Mag. Magn. Mat. **211**, 150 (2000).
- ¹⁷ A. K. Kar, A. Dhar, S. K. Ray, B. K. Mathur, D. Bhattacharya, and K. I. Chopra, J. Phys.: Cond. Matter **10**, 10795 (1998).
- ¹⁸ D.I. Savytskii, D. M. Trots, L. O. Vasylechko, N. Tamura and M. Berkowski, J. Appl. Cryst. **36**, 1197 (2003).
- ¹⁹ S. V. Kalinin and D. A. Bonnell, Phys. Rev. B **63**, 125411 (2001).
- ²⁰ Y. Ge, O. Heczko, O. Soderberg, and V. K. Lindroos, J. Appl. Phys. **96**, 2159 (2004).
- ²¹ G. Popov, S. V. Kalinin, T. Alvarez, T. J. Emge, M. Greenblatt, and D. A. Bonnell, Phys. Rev. B **65**, 064426 (2002).
- ²² J. P. Chapman, J. P. Attfield, L. M. Rodriguez-Martinez, L. Lezama, and T. Rojo, Dalton Trans. 3026 (2004).
- ²³ B. Dabrowski, X. Xiong, Z. Bukowski, R. Dybzinski, P. W. Klamut, J. E. Siewenie, O. Chmaissem, J. Shaffer, C. W. Kimball, J. D. Jorgensen, and S. Short, Phys. Rev. B **60**, 7006 (1999); X.

- Xiong, B. Dabrowski, O. Chmaissem, Z. Bukowski, S. Kolesnik, R. Dybziński, C. W. Kimball, and J. D. Jorgensen, *Phys. Rev. B* **60**, 10186 (1999).
- ²⁴ J. Geck, P. Wochner, S. Kiele, R. Klingeler, A. Revcolevschi, M. v. Zimmermann, B. Buchner, and P. Reutler, *New J. Phys.* **6**, 152 (2004).
- ²⁵ D. E. Cox, T. Iglesias, E. Moshopoulou, K. Hirota, K. Takahashi, and Y. Endoh, *Phys. Rev. B* **64**, 024431 (2001).
- ²⁶ M. Hervieu, A. Barnabe, C. Martin, A. Maignan, F. Damay, B. Raveau, *Eur. Phys. J. B* **8**, 31 (1999).
- ²⁷ J. Rodriguez-Carvajal, M. Hennion, F. Moussa, A. H. Moudden, L. Pinsard, and A. Revcolevschi, *Phys. Rev. B* **57**, R3189 (1998).
- ²⁸ G. L. Liu, J. S. Zhou, and J. B. Goodenough, *Phys. Rev. B* **70**, 224421 (2004).
- ²⁹ R. Klingeler, J. Geck, R. Gross, L. Pinsard-Gaudart, A. Revcolevschi, S. Uhlenbruck, and B. Buchner, *Phys. Rev. B* **65**, 174404 (2002).
- ³⁰ A. Asamitsu, Y. Moritomo, R. Kumai, Y. Tomioka, and Y. Tokura, *Phys. Rev. B* **54**, 1716 (1996).
- ³¹ A. N. Ulyanov, Seong-Cho Yu, and Dong-Seok Yang, private communication, unpublished.
- ³² P. G. Radaelli, G. Iannone, M. Marezio, H. Y. Hwang, S-W. Cheong, J. D. Jorgensen, D. N. Argyriou, *Phys. Rev. B* **56**, 8265 (1997).
- ³³ M. V. Lobanov, A. M. Balagurov, V. Ju. Pomjakushin, P. Fischer, M. Gutmann, A. M. Abakumov, O. G. D'yachenko, E. V. Antipov, O. I. Lebedev, and G. Van Tendeloo, *Phys. Rev. B* **61**, 8941 (2000)
- ³⁴ O. I. Lebedev, G. Van Tendeloo, A. M. Abakumov, S. Amelinckx, B. Leibold, and H.-U. Habermeier, *Phil. Mag. A* **79** 1461 (1999).
- ³⁵ M. Pissas, I. Margiolaki, G. Papavassiliou, D. Stamopoulos, and D. Argyriou, cond-mat/0503253 (unpublished).
- ³⁶ V. Markovich, G. Jung, Y. Yuzhelevski, G. Gorodetsky, A. Szewczyk, M. Gutowska, D. A. Shulyatev, and Ya. M. Mukovskii, *Phys. Rev. B* **70**, 64414 (2004).